# Measuring the cosmological background of relativistic particles with the Wilkinson Microwave Anisotropy Probe

Patrick Crotty

*Laboratoire de Physique Théorique LAPTH, Boîte Postal 110, F-74941 Annecy-le-Vieux Cedex, France*

Julien Lesgourgues

*Theory Division, CERN, CH-1211 Geneva 23, Switzerland*
*and Laboratoire de Physique Théorique LAPTH, Boîte Postal 110, F-74941 Annecy-le-Vieux Cedex, France*

Sergio Pastor

*Instituto de Física Corpuscular (CSIC-Universitat de València), Ed. Institutos de Investigación, Apdo. 22085, E-46071 Valencia, Spain*

We show that the first year results of the Wilkinson Microwave Anisotropy Probe (WMAP) constrain very efficiently the energy density in relativistic particles in the Universe. We derive new bounds on additional relativistic degrees of freedom expressed in terms of an excess in the effective number of light neutrinos $\Delta N_{\text{eff}}$. Within the flat $\Lambda$CDM scenario, the allowed range is $\Delta N_{\text{eff}} < 6$ (95% confidence level) using WMAP data only, or $-2.6 < \Delta N_{\text{eff}} < 4$ with the prior $H_0 = 72 \pm 8 \text{ km s}^{-1} \text{ Mpc}^{-1}$. When other cosmic microwave background and large scale structure experiments are taken into account, the window shrinks to $-1.6 < \Delta N_{\text{eff}} < 3.8$. These results are in perfect agreement with the bounds from primordial nucleosynthesis. Nonminimal cosmological models with extra relativistic degrees of freedom are now severely restricted.

## I. INTRODUCTION

What is the matter budget of the Universe? This fascinating and central question in cosmology is currently being answered with increasing precision, thanks to outstanding measurements of the cosmic microwave background (CMB) anisotropies, correlated with the study of large scale structure (LSS), of the primordial abundances of light elements, and many other observables in the far universe.

One of the most intriguing issues is to determine the contributions of matter and dark energy to the total energy density ($\Omega_m$ and $\Omega_\Lambda$ in units of the critical density). Inflation predicts $\Omega_m + \Omega_\Lambda = 1$ but, so far, there is no theoretical prediction on the value of each of these parameters. This explains why in most cosmological parameter analyses they receive much more attention than the radiation density $\Omega_r$, which is often assumed to be well known. However, the reference value of $\Omega_r$ relies on a strong theoretical prejudice: apart from the CMB photons, the dominant relativistic background would consist of the three families of neutrinos, whose temperature would be fixed with respect to the CMB temperature by the standard picture of neutrino decoupling prior to big bang nucleosynthesis (BBN).

Measuring the energy density of radiation today is not easy, because it is known to be three orders of magnitude below the critical density. The main constraints come either from the very early Universe, when radiation was the dominant source of energy, or from the observation of cosmological perturbations, which imprint the time of equality between matter and radiation. In particular, through BBN models, the primordial abundances of light elements can be related to $\Omega_r$, evaluated at the time when the mean energy in the universe was of order 1 MeV$^4$—while the power spectrum of photon anisotropies and of matter density carry a clear signature of the time at which $\Omega_r$ became comparable to $\Omega_m$, at energies of order $(0.1 \text{ eV})^4$. Until now, the BBN constraint on $\Omega_r$ was more stringent than the one from cosmological perturbations, by approximately one order of magnitude. This leaves the door wide open for various plausible assumptions concerning the radiation content of the Universe, which should not be necessarily the same during BBN and at the time of matter/radiation equality. For instance, a population of nonrelativistic particles may decay into relativistic ones, enhancing the radiation energy density. Moreover, the standard BBN scenario itself—which is the simplest way to explain the formation of light elements, but not the only one—needs to be tested. In this respect, the best would be to have some independent measurements of the two free parameters of BBN: the baryon density $\Omega_b h^2$ and the radiation density $\Omega_r h^2$ [where the reduced Hubble constant is $h \equiv H_0 / (100 \text{ km s}^{-1} \text{ Mpc}^{-1})$]. The later controls the expansion rate in the early universe. Some precise bounds on $\Omega_b h^2$ were already obtained from recent CMB experiments, while the determination of $\Omega_r h^2$ was still quite loose, compared to BBN predictions.

The goal of this paper is to update this analysis and to show that the outstanding data from the first year sky survey of the Wilkinson Microwave Anisotropy Probe (WMAP) [1,2] gives better constraints, showing increasing evidence in favor of standard BBN, and leaving very small room for extra relativistic degrees of freedom beyond the three neutrino flavors.

## II. THE EFFECTIVE NUMBER OF RELATIVISTIC NEUTRINOS

The energy density stored in relativistic species, $\rho_r$, is customarily given in terms of the so-called *effective number*

*of relativistic neutrino species* $N_{\text{eff}}$ (see Ref. [3] for a review and references), through the relation

$$\rho_{\text{r}} = \rho_\gamma + \rho_\nu + \rho_x = \left[ 1 + \frac{7}{8} \left( \frac{4}{11} \right)^{4/3} N_{\text{eff}} \right] \rho_\gamma, \qquad (1)$$

where $\rho_\gamma$ is the energy density of photons, whose value today is known from the measurement of the CMB temperature. Equation (1) can be also written as

$$N_{\text{eff}} \equiv \left( \frac{\rho_r - \rho_\gamma}{\rho_\nu^0} \right) \left( \frac{\rho_\gamma^0}{\rho_\gamma} \right), \qquad (2)$$

where $\rho_\nu^0$ denotes the energy density of a single species of massless neutrino with an equilibrium Fermi-Dirac distribution with zero chemical potential, and $\rho_\gamma^0$ is the photon energy density in the approximation of instantaneous neutrino decoupling. The normalization of $N_{\text{eff}}$ is such that it gives $N_{\text{eff}} = 3$ in the standard case of three flavors of massless neutrinos, again in the limit of instantaneous decoupling. In principle $N_{\text{eff}}$ includes, in addition to the standard neutrinos, a potential contribution $\rho_x$ from other relativistic relics such as majorons or sterile neutrinos.

It turns out that even in the standard case of three neutrino flavors the effective number of relativistic neutrino species is not exactly 3. The decoupling of neutrinos from the rest of the primordial plasma occurs at a temperature of 2–3 MeV, not far from temperatures of order the electron mass at which electron-positron annihilations transfer their entropy into photons, causing the well-known difference between the temperatures of relic photons and relic neutrinos, $T/T_\nu = (11/4)^{1/3}$ (see e.g. Ref. [4]). Accurate calculations [5–7] have shown that neutrinos are still slightly interacting with $e^\pm$, thus sharing a small part of the entropy release. This causes a momentum dependent distortion in the neutrino spectra from the equilibrium Fermi-Dirac behavior and a slightly smaller $T/T_\nu$ ratio. Both effects lead to a value of $N_{\text{eff}} = 3.034$. A further, though smaller, effect on $T/T_\nu$ is induced by finite temperature quantum electrodynamics (QED) corrections to the electromagnetic plasma [8,9]. A recent combined study of the incomplete neutrino decoupling and QED corrections concluded that the total effect corresponds to $N_{\text{eff}} = 3.0395 \simeq 3.04$ [10]. Therefore we define the extra energy density in radiation form as

$$\Delta N_{\text{eff}} \equiv N_{\text{eff}} - 3.04. \qquad (3)$$

The standard value of $N_{\text{eff}}$ corresponds to the case of massless or very light neutrinos, i.e. those with masses much smaller than 1 eV. More massive neutrinos affect the late evolution of the universe in a way that cannot be parametrized with a $\Delta N_{\text{eff}}$. However, the recent evidences of flavor neutrino oscillations in atmospheric and solar neutrinos, in particular after the recent KamLAND data show that the neutrino masses are not large enough, except in the case when the three mass eigenstates are degenerate (see e.g. Ref. [11] for a recent review). We do not consider such a case in the

present paper, but assume that the neutrino mass scheme is hierarchical, with the largest mass of order $m_\nu \simeq \sqrt{\Delta m_{\text{atm}}^2} \sim 0.05$ eV.

The value of $\Delta N_{\text{eff}}$ is constrained at the BBN epoch from the comparison of theoretical predictions and experimental data on the primordial abundances of light elements. Typically, the BBN bounds are of order $\Delta N_{\text{eff}} < 0.4 - 1$ [12–16]. Independent bounds on the radiation content of the universe can be extracted from the analysis of the power spectrum of CMB anisotropies. An enhanced contribution of relativistic particles delays the epoch of matter-radiation equality, which in turn increases the early integrated Sachs-Wolfe effect. Basically this leads to more power around the scale of the first CMB peak. Previous analyses found weak bounds on $\Delta N_{\text{eff}}$ [17–21], that can be significantly improved by adding priors on the age of the universe or by including supernovae and LSS data [22]. One of the most recent bounds on $N_{\text{eff}}$, from a combination of CMB and PSCz data [20], is $N_{\text{eff}} = 6^{+8}_{-4.5}$ (95% C.L.). Thus these bounds were not as restrictive as those from BBN. However, the precise measurements of the Wilkinson Microwave Anisotropy Probe (WMAP) (and those of Planck in the near future) are going to significantly improve the CMB constraint on $\Delta N_{\text{eff}}$, as shown in various forecast analyses (see for instance Refs. [23–25]) and in the calculations of this paper (see Sec. IV).

Many extensions of the standard model of particle physics predict additional relativistic degrees of freedom that will contribute to $\Delta N_{\text{eff}}$. There exist models with 4 neutrinos which include an additional sterile neutrino in order to explain the third experimental indication of neutrino oscillations [the Liquid Scintillator Neutrino Detector (LSND) results]. It was shown in many studies (see for instance Refs. [26,27]) that all four neutrino models, both of 2+2 and 3+1 type, lead to a full thermalization of the sterile neutrino flavor before BBN, and thus to $\Delta N_{\text{eff}} \simeq 1$, a value disfavored in the standard minimal model of BBN. Moreover, in these models there exists at least one neutrino state with mass of order 1 eV.

It is also possible that the relativistic degrees of freedom at the BBN and CMB epochs differ, for instance because of particle decays which increase the photon temperature relative to the neutrino one [28]. In some situations $\Delta N_{\text{eff}}$ can be effectively negative at BBN, such as the case of a distortion in the $\nu_e$ or $\bar{\nu}_e$ spectra [29,30], or a very low reheating scenario [31].

A nonstandard case that has been considered many times in the past is the existence of relic neutrino asymmetries, namely when the number of neutrinos and antineutrinos of the same flavor is significantly different. These so-called degenerate neutrinos are described by a dimensionless chemical potential $\xi_\alpha = \mu_{\nu_\alpha}/T$, and it has been shown that the neutrino energy density always increases for any value $\xi_\alpha \neq 0$:

$$\Delta N_{\text{eff}} = \sum_\alpha \left[ \frac{30}{7} \left( \frac{\xi_\alpha}{\pi} \right)^2 + \frac{15}{7} \left( \frac{\xi_\alpha}{\pi} \right)^4 \right]. \qquad (4)$$

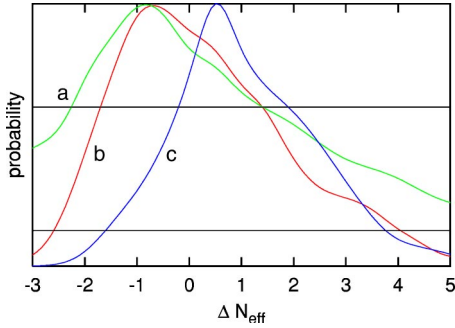Interestingly, some combinations of pairs $(\xi_e, \xi_{\mu,\tau})$ could

FIG. 1. The $\Delta N_{\rm eff}$ likelihood for WMAP+ weak $h$ prior (a/green), WMAP+strong $h$ prior (b/red), and the same plus other CMB experiments and the 2dF redshift survey (c/blue). The horizontal lines show the 68% (95%) confidence levels. The step of $\Delta N_{\rm eff}$ in our grid of models is 0.5.

still produce the primordial abundances of light elements for a larger baryon asymmetry, in the so-called degenerate BBN scenario [32]. At the same time, the weaker CMB bounds on $\xi_\nu$ are flavor blind [24,33]. However, it was recently shown that for neutrino oscillation parameters in the regions favored by atmospheric and solar neutrino data flavor equilibrium between all active neutrino species is established well before the BBN epoch [34–36]. Thus the stringent BBN bounds on $\xi_e$ apply to all flavors, so that the contribution of a potential relic neutrino asymmetry to $\Delta N_{\rm eff}$ is limited to very low values.

### III. METHOD

Using the CMBFAST code [37], we computed the cosmological perturbations [temperature and polarization anisotropies $C_l^{(T,E,TE)}$, matter power spectrum $P(k)$] for a grid of models with the following parameters: baryon density $\omega_b = \Omega_b h^2$, cold dark matter density $\omega_{\rm CDM} = \Omega_{\rm CDM} h^2$, hubble parameter $h$, scalar tilt $n_s$, optical depth to reionization $\tau$, global normalization—which is not discretized—and of course an additional contribution from relativistic particles

$\Delta N_{\rm eff}$. We include corrections to the CMB spectra from gravitational lensing [38], as computed by CMBFAST. Apart from $\Delta N_{\rm eff}$, our set of parameters is the simplest one used by the WMAP team in their parameter analysis [2], and accounts very well for the first year WMAP data. We restrict ourselves to a flat universe: since the curvature is known to be small from the position of the first CMB peak, we adopt the theoretical prejudice that the universe is exactly flat, as predicted by inflation, rather than almost flat. Therefore, $\Omega_\Lambda$ is equal to $1 - (\omega_b + \omega_{\rm CDM})/h^2$. Allowing for a small curvature could alter our results by a few percent. We also neglect the possible contribution of gravitational waves and a possible scale-dependent tilt. A running tilt, in favor of which the WMAP Collaboration finds some marginal evidence, would not change our predictions based on WMAP alone, because the later does not constrain the primordial spectrum on a wide enough range of scales. However, it could slightly alter our results based on CMB and LSS data.

Our grid (Fig. 1) covers the following ranges: $0.019 < \omega_b < 0.028$, $0.065 < \omega_{\rm CDM} < 0.27$, $0.5 < h < 0.9$, $0.8 < n_s < 1.28$, $0 < \tau < 0.5$, $-3 < \Delta N_{\rm eff} < 5$. We analyze it using an interpolation and minimization routine developed at LAPTH. Our code performs a multi-dimensional interpolation for each value of $C_l$ or $P(k)$ in order to obtain the spectrum at any arbitrary point, and then, computes the likelihood of the model. For WMAP, the likelihood is calculated using the software kindly provided at the NASA web site [39], and explained in Ref. [40]. We will also define a combined likelihood including the pre-WMAP CMB data compilation by Wang *et al.* [41] (which is still useful for constraining high multipoles), and the LSS data derived by Percival *et al.* [42] (32 points on wave numbers $k < 0.15h$ Mpc$^{-1}$) from the 2dF redshift survey [43]. For these two data sets, we use window functions and correlation matrices available from Refs. [44,45]. We constrain each free parameter using a Bayesian approach: the 68% (95%) confidence limits are defined as the values for which the marginalized likelihood drops by $\exp[-(\chi_0^2-1)/2]$ $(\exp[-(\chi_0^2-4)/2])$, where $\chi_0^2$ is the best chi square value in the whole parameter space.
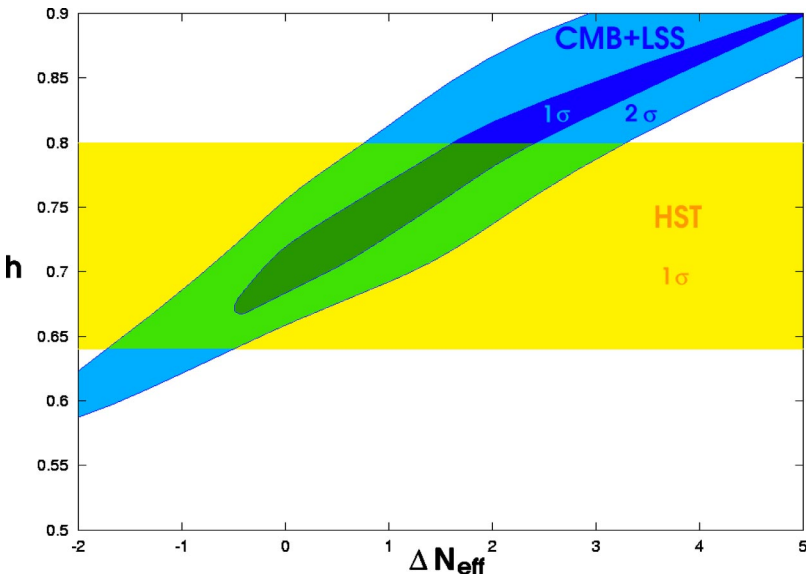


FIG. 2. The two-dimensional confidence limits on $(\Delta N_{\rm eff}, h)$, based on CMB and LSS data, at the 1-$\sigma$ (dark shading/dark blue) and 2-$\sigma$ (light shading/light blue) levels. The superimposed yellow stripe shows the HST Key Project measurement of $h$ (1-$\sigma$ level).

TABLE I. The best fit values and 2-$\sigma$ (95% C.L.) limits on $\Delta N_{\rm eff}$ for the different data sets.

| Data set | $\Delta N_{\rm eff}$ |
| --- | --- |
| WMAP+weak $h$ prior | $-0.9^{+6.9}_{-2.1}$ |
| WMAP+strong $h$ prior | $-0.7^{+4.7}_{-1.9}$ |
| WMAP+other CMB+LSS+strong $h$ prior | $0.5^{+3.3}_{-2.1}$ |

## IV. RESULTS AND DISCUSSION

We start the analysis using only the first year WMAP temperature and polarization data, plus a weak prior $0.5 < h < 0.9$, which is implicit from the limitation of the grid. We checked that for $\Delta N_{\rm eff}=0$, we find the same bounds as the WMAP collaboration, with a minimal effective chi square $\chi^2_{\rm eff}=1431.5$ for 1342 effective degrees of freedom (d.o.f.). The best fit over our whole grid has $(\Delta N_{\rm eff},\omega_b,h,\omega_{\rm CDM},\tau,n_s)=(-0.9,0.024,0.68,0.10,0.16,0.97)$, and a $\chi^2$ value which is not significantly lower ($\chi^2_{\rm eff}=1431.1$ for 1341 d.o.f.), showing that a nonzero $\Delta N_{\rm eff}$ is *not* required in order to improve the goodness of fit. At the 95% confidence level (C.L.), we can derive only an upper bound $\Delta N_{\rm eff}<6$, which is impressively smaller than the previous bound from CMB only, $\Delta N_{\rm eff}<14$ [20,25]. At the 1-$\sigma$ level, the extra relativistic energy density is limited to the range $-2.2<\Delta N_{\rm eff}<1.2$, corresponding to a dispersion of 3.4. This is in nice agreement with the prediction from Ref. [25] that with the full WMAP data, one would reach a dispersion of 3.17. The analysis reveals that the indetermination of this parameter is caused mainly by a degeneracy with $h$, as shown in previous works. When $\Delta N_{\rm eff}$ runs from $-3$ to 6, the best-fit value of $h$ goes from 0.55 to 0.90 (while $\omega_{\rm CDM}$ decreases, maintaining an approximately constant value of the matter fraction $\Omega_m=0.31\pm0.03$). After $\Delta N_{\rm eff}=6$, the weak prior $h<0.9$ is saturated, and the probability drops abruptly.

In order to remove the degeneracy, we add to the definition of the effective $\chi^2$ a Gaussian prior on $h$ derived from the Hubble Space Telescope (HST) Key Project [46], $h=0.72\pm0.08$ (at the 1-$\sigma$ level). This prior is sufficient to reduce significantly the 95% allowed window: $-2.6<\Delta N_{\rm eff}<4.0$. The no neutrino case with $\Delta N_{\rm eff}=-3$ is compatible with the data only beyond 99% C.L. The best-fit model has still a slightly negative $\Delta N_{\rm eff}=-0.7$, but this is not statistically significant. The best $\chi^2_{\rm eff}$ does not change very much (1431.1 for 1342 d.o.f.) because WMAP alone is in remarkable agreement with the Key Project value [2].

Finally, when we include the pre-WMAP data compilation and the 2dF redshift survey (i.e., information on the third and fourth CMB peak, and on the scale of the turn-over in the matter power spectrum), the window tends to shift a little bit towards positive values of $\Delta N_{\rm eff}$. The best-fit model has $\Delta N_{\rm eff}=0.5$ and $\chi^2_{\rm eff}=1492$ for 1396 d.o.f. The 95% allowed window is $-1.6<\Delta N_{\rm eff}<3.8$. Using all data, we find that the no neutrino case is excluded at 99.9% C.L., which constitutes a clear indication of the presence of relic background neutrinos, already shown by pre-WMAP data [20].

Note that throughout the analysis, we did not include any constraint from supernovae data. This is because all good-fitting models have naturally $(\Omega_m,\Omega_\Lambda)$ very close to (0.3,0.7). So, adding a supernovae prior would be completely irrelevant—unlike the $h$ prior, which plays a crucial role in removing the degeneracy with $\Delta N_{\rm eff}$. In order to emphasize this last point, we show in Fig. 2 the two-dimensional 1-$\sigma$ and 2-$\sigma$ confidence limits in $(\Delta N_{\rm eff},h)$ parameter space. The contours are based only on the CMB and LSS data (the HST Key Project result is just superimposed as a yellow stripe). The degeneracy between these two parameters clearly appears, showing that any improvement in the direct determination of $h$ will be crucial for closing the $\Delta N_{\rm eff}$ allowed window. For instance, large deviations from the standard value $\Delta N_{\rm eff}=0$ would be excluded if $h$ were measured to be very close to 0.70, while $h>0.75$ would bring strong evidence for extra relativistic species.

To summarize, we show in Table I the best fit values and 2-$\sigma$ (95% C.L.) limits on $\Delta N_{\rm eff}$ for the three different data sets. Our results show that the first year results of WMAP significantly improve the bounds on an additional contribution to the radiation density of the universe. In the near future, the updated data from WMAP and the new results from the Sloan Digital Sky Survey [47] should allow for an even better determination, providing a high-precision test of primordial nucleosynthesis.

*Note added.* After the submission of this work, our results were confirmed in Refs. [48] (with a generalization of the bounds to a nonflat Universe) and [49].

[1] C.L. Bennett *et al.*, astro-ph/0302207.
[2] D.N. Spergel *et al.*, astro-ph/0302209.
[3] A.D. Dolgov, Phys. Rep. **370**, 333 (2002).
[4] E.W. Kolb and M.S. Turner, *The Early Universe* (Addison-Wesley, New York, 1990).
[5] S. Hannestad and J. Madsen, Phys. Rev. D **52**, 1764 (1995).
[6] A.D. Dolgov, S.H. Hansen, and D.V. Semikoz, Nucl. Phys. **B503**, 426 (1997).
[7] S. Esposito *et al.*, Nucl. Phys. **B590**, 539 (2000).
[8] A.F. Heckler, Phys. Rev. D **49**, 611 (1994).
[9] R.E. Lopez and M.S. Turner, Phys. Rev. D **59**, 103502 (1999).
[10] G. Mangano, G. Miele, S. Pastor, and M. Peloso, Phys. Lett. B

**534**, 8 (2002).

[11] S. Pakvasa and J.W.F. Valle, hep-ph/0301061.

[12] E. Lisi, S. Sarkar, and F.L. Villante, Phys. Rev. D **59**, 123520 (1999).

[13] S. Esposito, G. Mangano, G. Miele, and O. Pisanti, J. High Energy Phys. **09**, 038 (2000).

[14] J.P. Kneller, R.J. Scherrer, G. Steigman, and T.P. Walker, Phys. Rev. D **64**, 123506 (2001).

[15] R.H. Cyburt, B.D. Fields, and K.A. Olive, Astropart. Phys. **17**, 87 (2002).

[16] A.R. Zentner and T.P. Walker, Phys. Rev. D **65**, 063506 (2002).

[17] G. Jungman, M. Kamionkowski, A. Kosowsky, and D.N. Spergel, Phys. Rev. D **54**, 1332 (1996).

[18] S. Hannestad, Phys. Rev. Lett. **85**, 4203 (2000).

[19] S. Esposito *et al.*, Phys. Rev. D **63**, 043004 (2001).

[20] S. Hannestad, Phys. Rev. D **64**, 083002 (2001).

[21] S.H. Hansen *et al.*, Phys. Rev. D **65**, 023511 (2002).

[22] W. Hu, D.J. Eisenstein, M. Tegmark, and M.J. White, Phys. Rev. D **59**, 023512 (1999).

[23] R.E. Lopez, S. Dodelson, A. Heckler, and M.S. Turner, Phys. Rev. Lett. **82**, 3952 (1999).

[24] W.H. Kinney and A. Riotto, Phys. Rev. Lett. **83**, 3366 (1999).

[25] R. Bowen *et al.*, Mon. Not. R. Astron. Soc. **334**, 760 (2002).

[26] P. Di Bari, Phys. Rev. D **65**, 043509 (2002).

[27] K.N. Abazajian, Astropart. Phys. **19**, 303 (2003).

[28] M. Kaplinghat and M.S. Turner, Phys. Rev. Lett. **86**, 385 (2001).

[29] A.D. Dolgov, S.H. Hansen, S. Pastor, and D.V. Semikoz, Nucl. Phys. **B548**, 385 (1999).

[30] S.H. Hansen and F.L. Villante, Phys. Lett. B **486**, 1 (2000).

[31] G.F. Giudice, E.W. Kolb, and A. Riotto, Phys. Rev. D **64**, 023508 (2001).

[32] H. Kang and G. Steigman, Nucl. Phys. **B372**, 494 (1992).

[33] J. Lesgourgues and S. Pastor, Phys. Rev. D **60**, 103521 (1999).

[34] A.D. Dolgov *et al.*, Nucl. Phys. **B632**, 363 (2002).

[35] Y.Y. Wong, Phys. Rev. D **66**, 025015 (2002).

[36] K.N. Abazajian, J.F. Beacom, and N.F. Bell, Phys. Rev. D **66**, 013008 (2002).

[37] U. Seljak and M. Zaldarriaga, Astrophys. J. **469**, 437 (1996).

[38] M. Zaldarriaga and U. Seljak, Phys. Rev. D **58**, 023003 (1998).

[39] NASA home page: http://lambda.gsfc.nasa.gov/

[40] L. Verde *et al.*, astro-ph/0302218.

[41] X. Wang, M. Tegmark, B. Jain, and M. Zaldarriaga, astro-ph/0212417.

[42] W.J. Percival *et al.*, astro-ph/0105252.

[43] E. Hawkins *et al.*, astro-ph/0212375.

[44] Max Tegmark's home page: http://www.hep.upenn.edu/~max

[45] 2dF home page: http://msowww.anu.edu.au/2dFGRS

[46] W.L. Freedman *et al.*, Astrophys. J. **553**, 47 (2001).

[47] SDSS Collaboration, J. Loveday, astro-ph/0207189.

[48] E. Pierpaoli, astro-ph/0302465.

[49] S. Hannestad, astro-ph/0303076.